行政院國家科學委員會專題研究計畫 期末報告

擴散波數平面磁振造影研究活體人腦胼胝體神經軸突尺寸與密度

計 畫 類 別 ：個別型
計 畫 編 號 ：NSC 101-2320-B-040-001-
執 行 期 間 ：101 年 08 月 01 日至 102 年 07 月 31 日
執 行 單 位 ：中山醫學大學醫學影像暨放射科學系

計 畫 主 持 人：翁駿程
共 同 主 持 人：曾文毅
計畫參與人員：碩士班研究生-兼任助理人員：洪于涵
碩士班研究生-兼任助理人員：林詩婷
大專生-兼任助理人員：林思妤
大專生-兼任助理人員：王惠瑜
大專生-兼任助理人員：王筑韻

報 告 附 件 ：出席國際會議研究心得報告及發表論文

公 開 資 訊 ：本計畫涉及專利或其他智慧財產權，2 年後可公開查詢

中 華 民 國 102 年 10 月 24 日

中文摘要：目的：胼胝體為連結大腦左右半腦的主要路徑，主要負責各種認知功能資訊的傳遞與處理，不同區域的胼胝體受到疾病進程發展、大腦認知功能、左右半腦交通損傷等因素影響，其結構會產生改變，包含軸突尺寸、軸突形狀。本研究提出前瞻性的擴散波數平面造影(q-planar imaging, QPI)來偵測活體人腦胼胝體的神經軸突尺寸與密度。

材料與方法：為了決定適用於臨床 3T MRI 機器之擴散波數平面造影最佳參數，即最大擴散敏感係數(bmax)與擴散波數空間取樣密度(Δq)，我們於一位正常健康受試者中作各種參數的取像比較，並得到最佳化的結果。有了最佳化的造影條件，14 位正常健康成年受試者將接受磁振造影掃瞄，我們以擴散權重面迴訊造影受試者大腦胼胝體正中矢狀切面，以 1009 個方向的擴散權重，即於最大擴散敏感係數(bmax = 5000 s/mm2)的二維擴散波數空間作 18 單位直徑圓形取樣(Δq = 0.0029 μm-1)。將擴散波數平面造影訊號先採用二維雙高斯曲面擬合分為快擴散與慢擴散二部分，經過二維 Fourier 轉換，可以得到水分子寬部分與窄部分擴散機率密度函數在影像切面的投影量，我們採用二維雙高斯曲面來估算擴散機率密度函數，並進一步獲得細胞外(extracellular)與細胞內(intracellular)平均位移量(mean displacement)與擴散機率(probability)，細胞內的結果可分別代表神經軸突尺寸與密度，結果將以已知的組織切片解剖作驗證。為了更視覺化呈現胼胝體正中矢狀切面神經軸突尺寸與密度分佈，我們採用 k-means 分群法來對擴散波數平面造影結果進一步分析。

結果：與已知組織切片解剖作比較，我們提出之前瞻性的擴散波數平面造影，配合最佳化造影參數可以偵測活體人腦胼胝體的神經軸突尺寸與密度，其中 genu 與 splenium 明顯較其它部分小與緻密。

結論：我們的結果顯示擴散波數平面造影新技術適用於一般臨床造影機器，並具有神經科學研究與臨床疾病診斷的潛力。

中文關鍵詞：擴散磁振造影、擴散波數平面造影、胼胝體、擴散機率、擴散位移量、神經軸突尺寸、神經軸突密度

英文摘要：Purpose: The corpus callosum (CC) is the main fiber tract interconnecting bilateral cerebral hemispheres, and is involved in a wide variety of cognitive functions Alteration of this fiber structure has been implicated in different mental disorders. However, an in vivo technique that can map axonal diameter and

axonal density of the CC is still lacking. Therefore, a new MRI method called q planar imaging (QPI) was proposed in which high density 2D diffusion encoding was performed on the mid sagittal plane of the CC.
Materials and Methods: To determine the optimal values of maximal diffusion sensitivity (bmax) and sampling density in the q space (Δq) for QPI on a clinical scanner, a heuristic estimation and an in vivo optimization study were performed on a healthy subject. Having known the optimal bmax and Δq, an in vivo validation study was performed on fourteen healthy subjects. The QPI data acquisition was performed on a 3T system using a diffusion-weighted spin echo EPI sequence. Multiple diffusion-weighted images were acquired corresponding to 1009 diffusion-encoding directions on a mid-sagittal plane of CC. The diffusion encoding directions corresponded to a set of 2D grid points confined in a circle with a radius of 18 increments (Δq = 0.0029 μm-1). The b values ranged from 0 to the optimal bmax (5000 s/mm2). The QPI data were decomposed into fast and slow components by bi-Gaussian fitting, and 2D Fourier transform was performed on the fast and slow components of the data to obtain broad (extracellular) and narrow (intracellular) components of the 2D probability density function (PDF) of molecular displacement, respectively. Two indices of water diffusion, mean displacement and the probability density at zero displacement, were computed from the 2D PDF at each pixel to map the axonal diameter and axonal density, respectively. Finally, k-means clustering analysis was performed to classify the indices automatically to confirm the consistency of the spatial patterns of the axonal density and axonal diameter in the CC.
Results: Compared with the know histology, QPI with optimum parameters produced reasonable distribution and segmentation of axonal diameter and density of the CC in normal human brain. The genu and splenium were significantly smaller and denser than those from other regions.
Conclusion: Our results showed that QPI was feasible

in clinical scanners, and might be potentially useful in neuroscience research and clinical application.

英文關鍵詞： diffusion magnetic resonance imaging, q-planar imaging, corpus callosum, probability, displacement, axonal diameter, axonal density

Introduction

The corpus callosum (CC) is the largest fiber tract that connects bilateral cerebral hemispheres, supporting inter-hemispheric connectivity. The callosal fibers connect different cortical regions of bilateral hemispheres which are thought to correspond to different cognitive functions. The CC can be unambiguously identified in the sagittal plane due to its large cross-sectional area. In view of the topographically-specific relation between sub-regions of the CC and the connected cortical regions, several partitioning schemes have been proposed to allow separate analysis of different sub-regions (Witelson 1985, Witelson 1989). Vertical partitions are commonly used which subdivide the CC into five sub-regions based on fractions of its maximal anterior-posterior length as proposed by Witelson (Witelson 1989). These sub-regions might be affected differently in the course of development, aging or disease. The altered distribution of axonal diameter and axonal density might be responsible for various cognitive impairments related to the connected cortical regions.

Background

The callosal fibers show different combinations of axonal diameter and axonal density at different sub-regions of the CC. In general, thin fibers are concentrated in the anterior part (genu) and posterior part (splenium) and relatively few in the middle part (body). Conversely, thick fibers are concentrated in the body and relatively few in the genu and splenium (Aboitiz, Scheibel et al. 1992). Being able to map axonal diameter and axonal density of the CC has the potential to assess the development of cerebral cortex, the status of a neurological disease and the inference of cognitive functions. Indeed, the distribution of the altered axonal diameters in the CC has been implicated in dyslexia (Njiokiktjien, de Sonneville et al. 1994, Hynd, Hall et al. 1995), autism (Piven, Bailey et al. 1997, Hughes 2007), schizophrenia (Randall 1983, Narr, Thompson et al. 2000, Rice and Barone 2000, Narr, Cannon et al. 2002, Brambilla, Cerini et al. 2005, Miyata, Hirao et al. 2007), Williams syndrome (Tomaiuolo, Di Paola et al. 2002, Luders, Di Paola et al. 2007), attention-deficit hyperactivity disorder (ADHD) (Giedd, Castellanos et al. 1994, Semrud-Clikeman, Filipek et al. 1994, Skranes, Vangberg et al. 2007), and bimanual function (Meyer, Roricht et al. 1998, Muetzel, Collins et al. 2008). Moreover, change in axonal diameters was found following exposure to alcohol and other toxic drugs (Livy and Elberger 2008).

Several diffusion MR techniques have been used to investigate the structural property of the white matter. One-dimensional q-space sampling with high sampling density and bandwidth, called q-space imaging (QSI), is used to obtain information about distribution of axonal diameters about the investigated materials (Stanisz, Szafer et al. 1997, Assaf, Blumenfeld-Katzir et al. 2008, Barazany, Basser et al. 2009, Ong and Wehrli 2010). Three-dimensional q-space sampling, diffusion spectrum imaging (DSI), is an alternative method to investigate the white matter structure. It probes the probability density function (PDF) of water molecular diffusion by sampling diffusion weighted images (DWI) in the 3D space of spatial modulation q (Wedeen, Hagmann et al. 2005). The requirements of very high field experimental systems or suffer from long acquisition times or high q-space sampling density make diffusion morphometry difficult to be implemented on clinical scanners.

Schneider et al. proposed a diffusion MR method that allow estimation of axonal diameter and density in the live human brain, and it significantly reduces scan time by making use of the a-priori known fiber orientation in structures with well defined single fiber organization like the corpus callosum (Schneider, Wheeler-Kingshott et al. 2010). Avram et al. reported a quadruple pulsed-field gradient (qPFG) diffusion MRI pulse sequence on a clinical scanner and demonstrated its ability to non-invasively detect average axonal diameters in the corpus callosum of healthy human volunteers (Avram, Ozarslan et al. 2013). The techniques of this kind assume a single axonal orientation in the tissue model, which may be a reasonable approximation only for the most coherently oriented brain white matter, such as the corpus callosum. Zhang et al. proposed a model which supports the simultaneous estimation of the axon diameter and orientation dispersion and provides an axonal diameter index that is robust to the presence of orientation dispersion (Zhang, Hubbard et al. 2011).

Purpose

Here, we proposed a technique called q-planar imaging (QPI) to map axonal diameter and axonal density in the mid-sagittal plane of the CC in vivo. This technique entails acquisition of a set of diffusion-weighted images by applying a set of diffusion-sensitive gradients in the same mid-sagittal plane of the

diffusion-encoding space (q space). The diffusion-sensitive gradients are applied in a way that the corresponding diffusion encoding vectors **q** are pointing at a set of grid points in the mid-saggital plane of the q space (q plane). The rationale is that the callosal fibers in the mid-sagittal plane are almost perpendicular to the mid-saggital plane. Therefore, QPI could provide the projection of the PDF onto this plane, and the information about axonal diameter and axonal density is fully retained without any compromise. Acquisition in the 2D q plane instead of the 3D q space allows us to acquire diffusion measurements densely populated in the q plane without prolonging the scan time. Furthermore, since only the mid-saggital plane of the CC is of interest, we only need to acquire QPI of a single slice, hence shortens the scan time further. Using QPI, it is possible to achieve a high density 2D q plane sampling from a clinical scanner within a reasonable amount of scan time.

Therefore, the goal of this study is twofold. First, we aimed to find the optimal values of QPI parameters, specifically the maximal diffusion sensitivity b_{max} and number diffusion measurements, to make QPI a clinically feasible technique. A heuristic estimation and an in vivo optimization study were performed on a healthy subject. Second, having known the optimal conditions, an in vivo validation study was performed on fourteen healthy subjects. The validation of QPI entailed comparison of the resulting spatial maps of axonal diameter and axonal density with the spatial distribution in known histology (Aboitiz, Scheibel et al. 1992).

Materials and Methods

In vivo study

The in vivo QPI study comprises two parts: an optimization study and a validation study. An optimization study was performed on a healthy subject (22 years old, male, right handedness) to determine the optimal imaging parameters for QPI. Using the optimal imaging parameters found in the optimization study, a validation study was performed on 14 healthy subjects (age: 22-32 years old, M/F: 9/5, all right handed). The QPI indices, i.e. full area at half maximum and probability density at zero displacement, were compared, respectively, with the axonal diameter and axonal density of the CC reported previously in a histological study (Aboitiz, Scheibel et al. 1992).

All subjects had no medical history of brain injury, psychiatric or neurological disorders. The study was approved by the Institutional Review Board, and the signed informed consent was obtained from the subjects before entering the study. The QPI experiment was performed on 3T MRI system (Tim Trio, Siemens MAGNETOM, Germany) with a 32-channel phased-array head coil. The pulse sequence was a diffusion-weighted echo-planar imaging (EPI) sequence with a twice-refocused balanced echo (Reese, Heid et al. 2003). QPI images were acquired in the mid-sagittal plane of the CC. They comprises different diffusion-weighted images acquired by applying different diffusion-encoding directions in the mid-sagittal plane of the CC.

Optimization study of QPI

According to the Fourier relationship between the diffusion encoding in the q space and the PDF in the real space, each of the encoding directions corresponded to a specific point on the mid sagittal plane in the q space or q plane. To determine the optimal b_{max}, 3 sets of QPI data were acquired with 3 different values of b_{max}, namely 3000, 5000, and 7000 s mm^{-2} based on the estimation results of b_{max}. We employed 1009 diffusion encoding directions corresponding to a set of grid points in the q space that were located within a circle of 18 units on the q-plane. The diffusion sensitivities (b values) changed from 0 to b_{max} according to the locations of the diffusion encodings in the q space. The imaging parameters were TR/TE = 800/119~160 ms, spatial resolution = 1.7 x 1.7 x 10 mm^3 and NEX = 1. The total scanning time was about 40 minutes.

In the previous estimation, required q should be smaller than 0.013 m^{-1}. Using typical QPI parameters, we found that q used was in the range of 0.00242 ~ 0.00577 m^{-1}, 2 ~ 5 times smaller than 0.013 m^{-1}. Therefore, in this optimization study, 3 different q's were tested under the same b_{max} of 5000 s mm^{-2}. Three different q's (0.0033, 0.00347 and 0.00521 m^{-1}) were tested by setting three different diffusion encoding directions (317, 709 and 1009 directions, respectively) corresponding to three different numbers of increment from 0 to q_{max} (10, 15 and 18, respectively). To control for signal-to-noise ratio, NEX = 3, 2, and 1 were used for 317, 709 and 1009 diffusion encodings, respectively. The imaging parameters were TR/TE = 800/142 ms and spatial resolution = 1.7 x 1.7 x 10 mm^3. The total scan time for the 3 sets of QPI was about 45 minutes.

Validation study of QPI

According to the results of the optimization study, 1009 diffusion-encodings and b_{max} = 5000 s mm^{-2} were determined to be the optimum for the QPI data acquisition. Imaging parameters were TR/TE = 1000/142 ms, in-plane resolution = 1.7 mm, slice thickness = 10 mm and NEX = 1. The total scan time for the QPI study was about 17 minutes. In addition to QPI, multiple slices of T2-weighted (T2W) images were acquired using a fast spin echo sequence with in-plane resolution = 0.55 mm and slice thickness = 2.5 mm.

QPI analysis

According to the Fourier relationship between the signal intensity in the q space and the PDF in the real space (Wedeen, Hagmann et al. 2005), 2D Fourier transform of the signal intensity acquired in the q plane is the projection of the 3D displacement probability distribution onto the mid-sagittal plane. To compute the projected displacement probability distribution, the 2D signal decay of the diffusion data in the q-plane was first fitted with a 2D bi-Gaussian function, and the two Gaussian curved surfaces of signal decay were then obtained (i.e. slow and fast components). To perform 2D bi-Gaussian fitting, the turning point of the signal decay was first found. The round mask with radius equaled to the turning point was used to remove the signal from low q plane, and an asymmetric Gaussian curved surface was used to fit the slow component. Then the fast component was obtained by subtracting the slow Gaussian curved surface from the total signal decay, and another asymmetric Gaussian curved surface was used to fit the fast component. We performed 2D Fourier transformation of the slow and fast Gaussian curved surfaces of signal decay with respect to the q values (without any smoothing) which produced two Gaussian curved surfaces of displacement probability (i.e. narrow and broad components). The narrow Gaussian referred to restrictive diffusion in the intracellular compartment, whereas the broad Gaussian referred to hindered diffusion in the extracellular compartment (Assaf and Cohen 1998). Here we assumed that there was no exchange of water molecules between the two compartments.

The 2D narrow Gaussian can be plotted as a curved surface of displacement probability, and the mean displacement was estimated by computing the full area at half maximum of the displacement probability,

which provided information about relative axonal diameters of callosal fibers (Assaf, Mayk et al. 2000). The full area at half maximum was calculated by counting the numbers of probability values of the distribution which were higher than a half of the maximal probability. Another index, the probability density at zero displacement, was also determined by deriving the value of the probability density at the origin, which provided the information about relative axonal density (Assaf, Mayk et al. 2000). In the same way, mean displacement and probability density at zero displacement were extracted from the broad Gaussian to provide the information about relative size and density of the extracellular space.

After obtaining the indices of the mean displacement (full area at half maximum of the narrow Gaussian displacement probability), the probability density at zero displacement of the narrow Gaussian of each pixel of the CC, the individual values of each index were normalized to their own means for group comparison. The extracellular space and density information extracted from the broad Gaussian curved surfaces of displacement probability distribution were also calculated and discussed.

Partitioning schemes for CC

Witelson's partitioning method was used to subdivide the CC into five regions according to fractions of its maximal anterior-posterior length (Fig. 1) (Witelson 1989), namely rostrum and genu (CC1), anterior body (CC2), posterior body (CC3), isthmus (CC4) and splenium (CC5). The mean index within each of the five regions was then calculated and compared to Aboitiz's histological study on the distribution of standard axonal diameter and axonal density (Aboitiz, Scheibel et al. 1992). For the optimization study, Aboitiz's distribution of standard axonal diameter and axonal density was also used to compare with the distributions of the indices derived from the QPI. The optimal values of b_{max} and of number of diffusion encodings were determined by finding the condition that was closest to the known distribution obtained from Aboitiz's study.

K-means clustering and statistical analysis

In order to visualize the axonal density and diameter distribution pattern along the corpus callosum, we used a clustering algorithm (k-means with correlation as the distance measure) with QPI indices, i.e. the probability at zero displacement and the mean displacement of narrow Gaussian displacement probability, as inputs. Each pixel in each cluster was regarded as an individual observation. The number of clusters (k) was

incremented until no additional information was observed, and finally was set to six clusters, one of which was assigned outlier pixels. The data were tested for statistical significance using a repeated measure analysis of variance (ANOVA) with the clusters as the independent factor.

Results

2D curve surfaces and 2D contours

To compute the projected displacement probability distribution, the 2D signal decay of the diffusion data in the q-plane was first fitted with a 2D bi-Gaussian function, and the two Gaussian curved surfaces of signal decay were then obtained (i.e. slow and fast components). Figure 2a and 2b demonstrated the 2D curve surfaces of the signal decay in the q-plane for slow and fast components, respectively. Five curve surfaces in a row were the averaged signal decay calculated from the five segments of mid-sagittal CC. 2D Fourier transformation of the slow and fast Gaussian curved surfaces of signal decay with respect to the q values was then performed to produced two Gaussian curved surfaces of displacement probability (i.e. narrow and broad components). Figure 2c and 2d demonstrated the 2D curve surfaces of the projected probability distribution function (PDF) for narrow (intracellular space) and broad (extracellular space) components, respectively. Five curve surfaces in a row were the averaged PDF calculated from the five segments of mid-sagittal CC.

QPI optimization

Probability density at zero displacement and mean displacement derived from the narrow (intracellular) Gaussian component were rendered in color maps. Figure 3a shows the maps acquired with different values of b_{max} (3000, 5000 and 7000 s mm^{-2}) and the same diffusion encoding direction of 1009. Figure 3b shows the maps acquired with different numbers of diffusion encodings (317, 709, 1009) and the same b_{max} of 5000 s mm^{-2} (Fig. 3b). By visual inspection, we can see that CC5 shows higher probability (implying higher axonal density) than other parts of CC, and CC1 and CC5 show lower displacement (implying smaller axonal diameter) than the middle part of CC (CC2, CC3 and CC4).

Figure 4e and 4f show the distribution patterns of mean axonal density and axonal diameter investigated by Aboitiz et al. (Aboitiz, Scheibel et al. 1992). The histological analysis of Aboitiz et. al. demonstrate three

key features. 1) Axons with a diameter larger than 3 μm are only found in the body of the corpus callosum. 2) Axons with a diameter smaller than 0.4 μm are only found in the genu and splenium of the corpus callosum. 3) Axon density and uniformity tend to be higher at genu and splenium compared to the body. These two distribution patterns are used as a reference standard for comparison to the distribution patterns of the probability at zero displacement and the mean displacement acquired with different values of b_{max}, i.e. 3000, 5000 and 7000 s mm^{-2} (Fig. 4a and 4b). The plots show that b_{max} of 5000 s mm^{-2} or 7000 s mm^{-2} are better than b_{max} of 3000 s mm^{-2} because their distribution patterns match closer to Aboitiz's patterns. Consider lower requirements of the gradient power, we chose b_{max} of 5000 s mm^{-2} as the optimal value in the following study for the optimal number of diffusion encoding directions.

Figure 5a and 5b show the distribution patterns of the probability at zero displacement and the mean displacement acquired with different numbers of diffusion encodings (317, 709 and 1009). Comparing with Aboitiz's patterns, there is no significant difference among the diffusion encoding numbers. Consider shorter scan time, the 1009 sampling points with 1 NEX is a better choice than 709 with 2 NEX and 317 with 3 NEX. Therefore, b_{max} = 5000 s/mm^2 and 1009 sampling points with 1 NEX were chosen for the in vivo validation study. The size and density of the extracellular space were also calculated from the broad Gaussian components (Fig. 4c, 4d, 5c and 5d).

QPI in human CC

Figure 6 shows two representative datasets from two subjects (one male and one female) including the different estimate parameters from QPI analysis. Figure 6a shows mid-saggital T2-weighted MRI. Figure 6b and 6c show, respectively, the maps of the probability density at zero displacement and the mean displacement derived from the narrow Gaussian component. We can see that the maps of these two indices provide spatial distribution of the axonal density and axonal diameter in the CC.

Figure 7 shows the distribution patterns averaged over the 14 subjects. Figure 7a and 7b are, respectively, the probability density at zero displacement and mean displacement derived from the narrow (intracellular) Gaussian component. Figure 7c and 7d are the same plots derived from the broad (extracellular) Gaussian

component. The distribution patterns derived from the narrow Gaussian component agree well with Aboitiz's patterns, showing relatively higher axonal density and smaller axonal diameter at CC1 and CC5. In the patterns derived from the broad Gaussian component, the probability density at zero displacement is rather constant from CC1 to CC5, whereas the mean displacement moderately agrees with that of the narrow Gaussian. The results imply that the density of the extracellular space is rather uniform across all CC regions, whereas the size of the extracellular space has a distribution pattern similar to that of axonal diameter. Our results agree with Aboitiz's results in postmortem histological study (Aboitiz, Scheibel et al. 1992).

Cluster analysis of the axonal diameter and density distribution

To classify different clusters of axonal density and axonal diameter automatically, cluster analysis was performed to segment the CC based on two QPI indices, the probability density at zero displacement and the mean displacement derived from the narrow Gaussian. Six clusters were assigned as the input, one of which represents noise or outliers. The remaining five clusters represented the five segments emerged from the analysis. Figure 8 shows the analysis results in four different subjects (2 male and 2 female). In general, the cluster analysis separates the CC into four major divisions, namely genu, body, isthmus and splenium. In the maps of the probability density at zero displacement (Fig. 8a - d), the red cluster corresponds to the genu, the green and blue clusters correspond to the body, the yellow cluster corresponds to the isthmus, and the brown cluster corresponds to the splenium. In the maps of the mean displacement (Fig. 8e - h), the green cluster corresponds to the genu, the red and brown clusters correspond to the body, the yellow cluster corresponds to the isthmus, and the blue cluster corresponds to the splenium. The results also agrees with Aboitiz's results (Aboitiz, Scheibel et al. 1992).

Discussions

This study presents a diffusion MRI technique, QPI, for *in vivo* mapping of axonal diameter and axonal density of the corpus callosum. The mean displacement and the probability density at zero displacement derived from the QPI data provide a new contrast indicating relative axonal diameter and axonal density which are beyond the existing contrast in current MRI techniques. Moreover, the scan time of 17 min makes clinical study highly feasible. QPI, as a tool for measuring the axonal diameter and axonal density, has all

the advantages of other diffusion MRI based methods such as non-invasiveness and acceptable scan time. Conventional measurement of the axonal diameter and axonal density requires sacrificing the animal and excising, fixing, sectioning, staining and image processing only a small portion of the tissue sample. QPI can probe large tissue regions without being a propensity to histological preparation artifacts. Because the measurement is inherently noninvasive, it can also be performed longitudinally on the same subject, possibly using different scanners at different centers. However, QPI has some limitations just like any other diffusion MRI based method. More details were addressed below (Limitations).

Potential neuroscience impact

The information of QPI could have a significant impact on the white matter architecture, structural connectivity, and even functional connectivity. Although QPI measures a morphological parameter of the tissue, in neuroscience morphology and function are linked therefore the ability to estimate or measure fine morphological features may imply on the functionality of the tissue. Using this concept, QPI may help to advance our knowledge on neuroanatomical changes occurring in white matter disorders, changes occurring in white matter during normal and abnormal development, and the functional deficits that occur in various brain diseases and disorders. For example, QPI would provide a means of testing hypotheses that the axonal diameter and density distribution changes in diseases and developmental disorders. QPI could also provide additional information for white matter tractography, especially at junctions where fibers cross or kiss. For instance, in the assumption that fiber remains continuous through such a junction, we can impose the continuity of the parameters characterizing the axonal diameter distribution to determine which branches are connected through such a junction.

The proportion of intracellular and extracellular space and density

Our results showed not only the distribution patterns of the size and the density of the intracellular and the extracellular components along human CC, but also the proportion of intracellular and extracellular space and density (Fig. 7). The fraction of intracellular density in CC was about 10 times higher than extracellular density (Fig. 7a, c). The water molecule in the extracellular could probe about 25 times longer in distance than it in the intracellular space (Fig. 7b, d). Although the results were various depended on the different

parts of CC, it agree with Aboitiz's results in postmortem histological study (Aboitiz, Scheibel et al. 1992). This implies that QPI can provide not only intracellular and extracellular information, but also the relationship between two compartments.

Partitioning schemes for CC

Numerous approaches have been proposed to subdivide the CC into several geometric partitions, including sectioning the CC according to its specific fractions of the maximal anterior-posterior length (Witelson 1989, Duara, Kushch et al. 1991), particular angular rays from the callosal centroid (Weis, Kimbacher et al. 1993), and several rays normal to a series of equidistant nodes on the ventral callosal boundary (Clarke and Zaidel 1994, Rajapakse, Giedd et al. 1996, Stievenart, Iba-Zizen et al. 1997). The most recommendable method is Witelson partitioning scheme (Witelson 1989), which divides the CC along its first principal axis (FPA), roughly corresponding to the longest axis of the outline. For five subregions, four division points need to be defined. These are referenced along the FPA, ranging from zero, the anterior CC part, to one, the posterior part. In Witelson's original study, division points are [1/3, 1/2, 2/3, 4/5] (Witelson 1989).

QPI and other diffusion indices

A variety of MR techniques have been proposed to investigate the morphology and microstructural organization of the human brain non-invasively (Allen, Richey et al. 1991). Novel approaches make use of the characteristic T2 relaxation times for the different water compartments in tissue, by which the myelin content can be inferred *in vivo* (MacKay, Whittall et al. 1994, Laule, Vavasour et al. 2007). The method is limited by the long scan time and limited spatial coverage. An alternative approach is to isolate myelin-water using linear combination filtering of several conventional spin echo images and express it as a fraction of the total water content to generate myelin-water fraction (MWF) images (Brosnan, Wright et al. 1988, Jones, Xiang et al. 2004, Vidarsson, Conolly et al. 2005). Diffusion tensor imaging (DTI) provides a measure of the magnitude and orientation of water self-diffusion to characterize, respectively, the microstructure integrity and connectivity of the white matter (Basser, Mattiello et al. 1994). Typical scalar quantities obtained from DTI include the mean diffusivity (MD), a measure of the directionally invariant magnitude of diffusion, axial ($\lambda_{\parallel}$) and radial diffusivity ($\lambda_{\perp}$), which quantify the magnitude of diffusion parallel and orthogonal to

the principal direction of water diffusion, and relative or fractional anisotropy (FA), which represents the degree of anisotropy within a voxel of tissue (Chepuri, Yen et al. 2002, Hofer and Frahm 2006). Combined with an extension of DTI and tractography, fiber density index (FDi) provides an indirect measure of the number of fiber paths traversing a region of interest (ROI), which can measure the microstructural composition of neural fibers, such as myelin content (Roberts, Liu et al. 2005, Liu, Vidarsson et al. 2010).

The CC fiber properties of the subdivisions have been evaluated using diffusion quantitative indices, such as FA and MD (Chepuri, Yen et al. 2002, Hofer and Frahm 2006). In QPI, probability map qualified the fiber density, which was similar to DA, FA, FDi and MWF, and displacement map described the relative axonal diameter distribution, which was closed to MSL, MD and $\lambda_{\perp}$.

Limitations

As a diffusion based framework, QPI is limited in the range of experimental diffusion times and length scales that it can probe. A specific limitation of QPI is the need to observe displacements exactly perpendicular to the fiber direction. Applying QPI on other fiber systems is possible by knowing a priori the path of the fibers, such as from DTI based tractography. With bi-Gaussian method, QPI so far could provide qualitative information of relative fiber density (probability map of narrow Gaussian displacement distribution) and axonal diameter distribution (displacement map of narrow Gaussian distribution). However, QPI may or may not apply in all white matter regions, where for example, compartmental exchange may be important. This is also one of the reasons we did not calculate the absolute value of axonal size and density. More complex model which takes intracellular and extracellular water molecular interaction and exchange, permeability of cell membrane and ion channels into consideration is needed for the quantitative results. Instead of absolute quantification, the axonal density and axonal diameter distributions are able to be used to segment tissue by k-means clustering analysis, which is similar to atlasing via cytoarchitecture. Although bi-Gaussian method was used in this paper to distinguish intracellular information from extracellular space, it does not separate the thin and thick axonal fibers in the C.C. The results are merely the averaged axonal diameter and axonal density of these two types of fibers. Differentiation of thin and thick fibers would require further modeling of the restricted diffusion signal.

Conclusion

We propose the QPI method with bi-Gaussian fitting to map the distribution of relative axonal diameters and density in human CC. The effects of different parameters of imaging were also discussed. Our results are consistent with the previous reports. Being a diffusion MRI-based methodology, our results demonstrate the feasibility of QPI on clinical scanners, and show the potential for morphometric mapping of callosal fibers in disease brains.

References

Aboitiz, F., A. B. Scheibel, R. S. Fisher and E. Zaidel (1992). "Fiber composition of the human corpus callosum." Brain Res **598**(1-2): 143-153.

Allen, L. S., M. F. Richey, Y. M. Chai and R. A. Gorski (1991). "Sex differences in the corpus callosum of the living human being." J Neurosci **11**(4): 933-942.

Assaf, Y., T. Blumenfeld-Katzir, Y. Yovel and P. J. Basser (2008). "AxCaliber: a method for measuring axon diameter distribution from diffusion MRI." Magn Reson Med **59**(6): 1347-1354.

Assaf, Y. and Y. Cohen (1998). "Non-mono-exponential attenuation of water and N-acetyl aspartate signals due to diffusion in brain tissue." J Magn Reson **131**(1): 69-85.

Assaf, Y., A. Mayk and Y. Cohen (2000). "Displacement imaging of spinal cord using q-space diffusion-weighted MRI." Magn Reson Med **44**(5): 713-722.

Avram, A. V., E. Ozarslan, J. E. Sarlls and P. J. Basser (2013). "In vivo detection of microscopic anisotropy using quadruple pulsed-field gradient (qPFG) diffusion MRI on a clinical scanner." Neuroimage **64**: 229-239.

Barazany, D., P. J. Basser and Y. Assaf (2009). "In vivo measurement of axon diameter distribution in the corpus callosum of rat brain." Brain **132**(Pt 5): 1210-1220.

Basser, P. J., J. Mattiello and D. LeBihan (1994). "MR diffusion tensor spectroscopy and imaging." Biophys J **66**(1): 259-267.

Brosnan, T., G. Wright, D. Nishimura, Q. Z. Cao, A. Macovski and F. G. Sommer (1988). "Noise reduction in magnetic resonance imaging." Magn Reson Med **8**(4): 394-409.

Chepuri, N. B., Y. F. Yen, J. H. Burdette, H. Li, D. M. Moody and J. A. Maldjian (2002). "Diffusion anisotropy in the corpus callosum." AJNR Am J Neuroradiol **23**(5): 803-808.

Clarke, J. M. and E. Zaidel (1994). "Anatomical-behavioral relationships: corpus callosum morphometry and hemispheric specialization." Behav Brain Res **64**(1-2): 185-202.

Duara, R., A. Kushch, K. Gross-Glenn, W. W. Barker, B. Jallad, S. Pascal, D. A. Loewenstein, J. Sheldon, M. Rabin, B. Levin and et al. (1991). "Neuroanatomic differences between dyslexic and normal readers on magnetic resonance imaging scans." Arch Neurol **48**(4): 410-416.

Hofer, S. and J. Frahm (2006). "Topography of the human corpus callosum revisited--comprehensive fiber tractography using diffusion tensor magnetic resonance imaging." Neuroimage **32**(3): 989-994.

Jones, C. K., Q. S. Xiang, K. P. Whittall and A. L. MacKay (2004). "Linear combination of multiecho data: short T2 component selection." Magn Reson Med **51**(3): 495-502.

Laule, C., I. M. Vavasour, S. H. Kolind, D. K. Li, T. L. Traboulsee, G. R. Moore and A. L. MacKay (2007). "Magnetic resonance imaging of myelin." Neurotherapeutics **4**(3): 460-484.

Liu, F., L. Vidarsson, J. D. Winter, H. Tran and A. Kassner (2010). "Sex differences in the human corpus callosum microstructure: A combined T(2) myelin-water and diffusion tensor magnetic resonance imaging study." Brain Res.

MacKay, A., K. Whittall, J. Adler, D. Li, D. Paty and D. Graeb (1994). "In vivo visualization of myelin water in brain by magnetic resonance." Magn Reson Med **31**(6): 673-677.

Ong, H. H. and F. W. Wehrli (2010). "Quantifying axon diameter and intra-cellular volume fraction in excised mouse spinal cord with q-space imaging." Neuroimage **51**(4): 1360-1366.

Rajapakse, J. C., J. N. Giedd, J. M. Rumsey, A. C. Vaituzis, S. D. Hamburger and J. L. Rapoport (1996).

"Regional MRI measurements of the corpus callosum: a methodological and developmental study." Brain Dev **18**(5): 379-388.

Reese, T. G., O. Heid, R. M. Weisskoff and V. J. Wedeen (2003). "Reduction of eddy-current-induced distortion in diffusion MRI using a twice-refocused spin echo." Magn Reson Med **49**(1): 177-182.

Roberts, T. P., F. Liu, A. Kassner, S. Mori and A. Guha (2005). "Fiber density index correlates with reduced fractional anisotropy in white matter of patients with glioblastoma." AJNR Am J Neuroradiol **26**(9): 2183-2186.

Schneider, T., C. A. Wheeler-Kingshott and D. C. Alexander (2010). "In-vivo estimates of axonal characteristics using optimized diffusion MRI protocols for single fibre orientation." Med Image Comput Comput Assist Interv **13**(Pt 1): 623-630.

Stanisz, G. J., A. Szafer, G. A. Wright and R. M. Henkelman (1997). "An analytical model of restricted diffusion in bovine optic nerve." Magn Reson Med **37**(1): 103-111.

Stievenart, J. L., M. T. Iba-Zizen, A. Tourbah, A. Lopez, M. Thibierge, A. Abanou and E. A. Cabanis (1997). "Minimal surface: a useful paradigm to describe the deeper part of the corpus callosum?" Brain Res Bull **44**(2): 117-124.

Vidarsson, L., S. M. Conolly, K. O. Lim, G. E. Gold and J. M. Pauly (2005). "Echo time optimization for linear combination myelin imaging." Magn Reson Med **53**(2): 398-407.

Wedeen, V. J., P. Hagmann, W. Y. Tseng, T. G. Reese and R. M. Weisskoff (2005). "Mapping complex tissue architecture with diffusion spectrum magnetic resonance imaging." Magn Reson Med **54**(6): 1377-1386.

Weis, S., M. Kimbacher, E. Wenger and A. Neuhold (1993). "Morphometric analysis of the corpus callosum using MR: correlation of measurements with aging in healthy individuals." AJNR Am J Neuroradiol **14**(3): 637-645.

Witelson, S. F. (1985). "The brain connection: the corpus callosum is larger in left-handers." Science **229**(4714): 665-668.

Witelson, S. F. (1989). "Hand and sex differences in the isthmus and genu of the human corpus callosum. A postmortem morphological study." Brain **112 (Pt 3)**: 799-835.

Zhang, H., P. L. Hubbard, G. J. Parker and D. C. Alexander (2011). "Axon diameter mapping in the presence of orientation dispersion with diffusion MRI." Neuroimage **56**(3): 1301-1315.

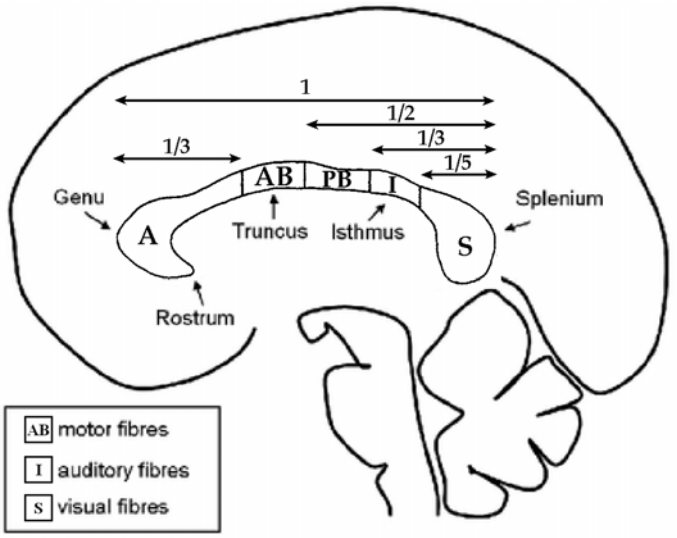

Figure 1 Witelson's partitioning schemes for regional analysis of human corpus callosum which subdivide the callosum into five regions based on fractions of its maximal anterior-posterior length, namely rostrum and genu (CC1), anterior body (CC2), posterior body (CC3), isthmus (CC4) and splenium (CC5).

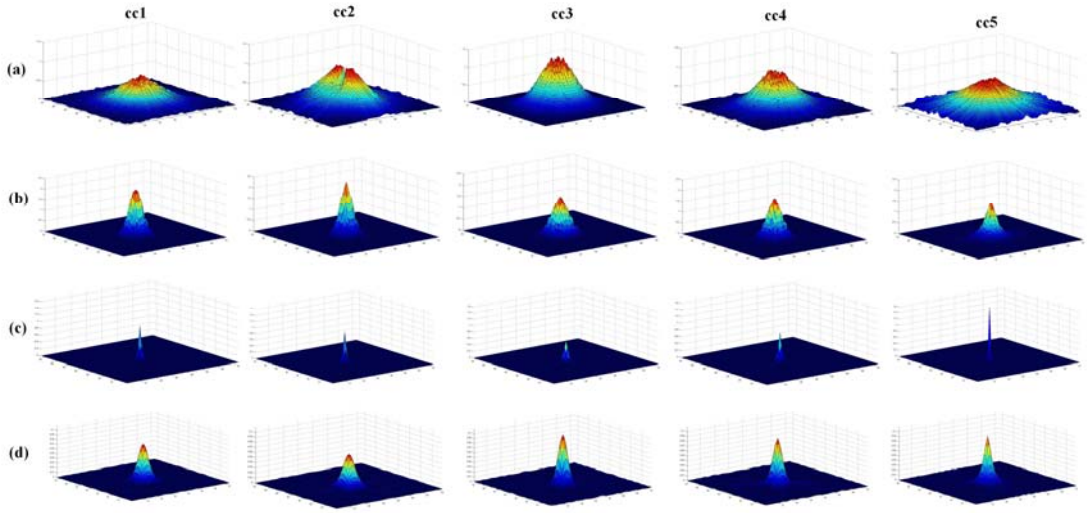

Figure 2 (a, b) 2D curve surfaces of the mean signal decay in the q-plane and (c, d) 2D curve surfaces of the mean projected probability distribution function (PDF) after 2D Fourier transform along the human CC. Five curve surfaces in a row were the averaged signal decay and averaged PDF calculated from the five segments of mid-sagittal CC. (a) Slow and (b) fast components calculated from the averaged bi-Gaussian decay curve surfaces of CC in all normal subjects (n=14). (c) Narrow (intracellular space) and (d) broad (extracellular space) components calculated from the averaged bi-Gaussian displacement distribution of CC in all normal subjects (n=14). The units in probability and displacement were arbitrary values.

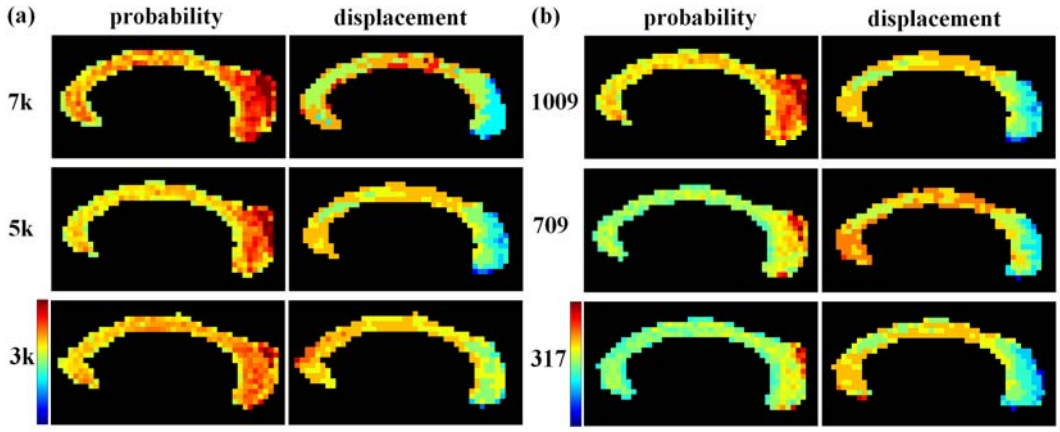

Figure 3 Sagittal CC maps of probability and displacement of narrow Gaussian displacement distribution with different (a) cutoff b-values and (b) sampling numbers in q-plane.

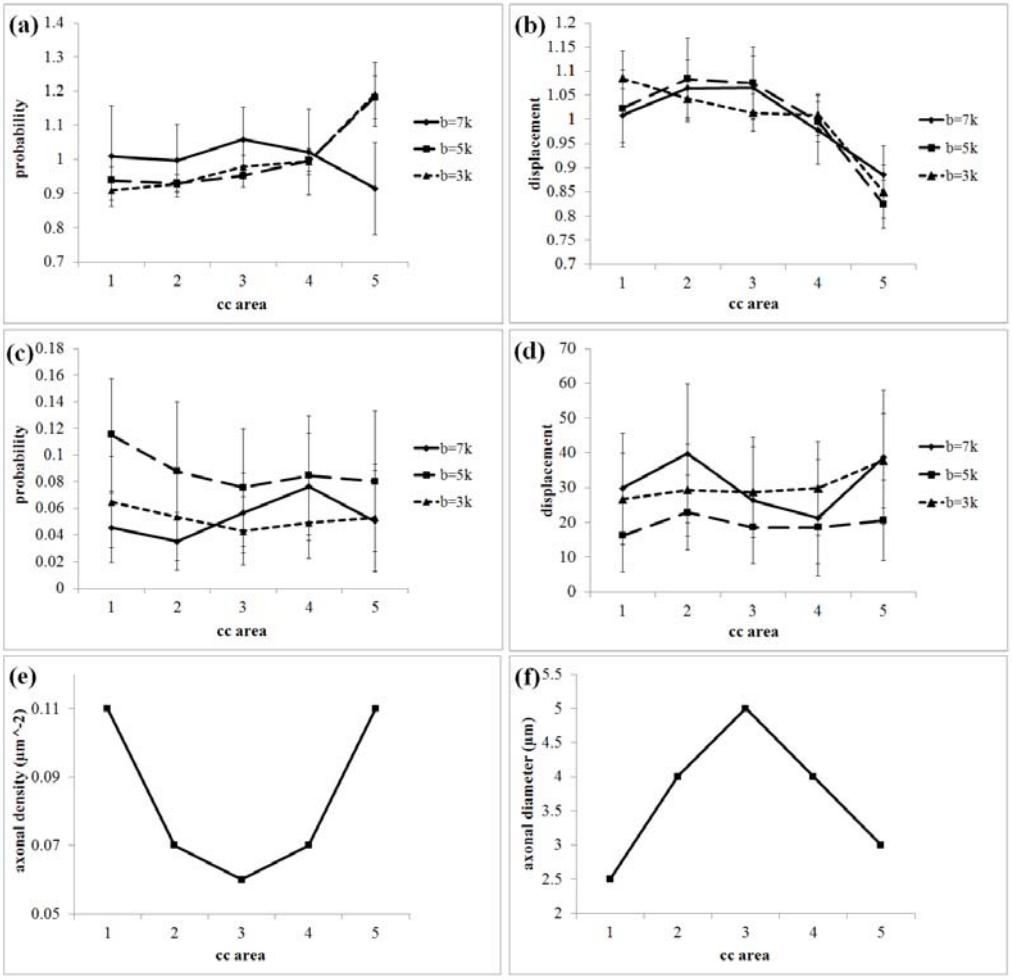

Figure 4 (a) Probability and (b) displacement distribution of CC calculated from narrow Gaussian displacement distribution with different cutoff b-values and the same sampling q-points. (c) Probability and (d) displacement distribution of CC calculated from broad Gaussian displacement distribution with different cutoff b-values and the same sampling q-points. (e) Mean axonal density and (f) mean axonal diameter of human CC found by histology (Aboitiz, Scheibel et al. 1992).

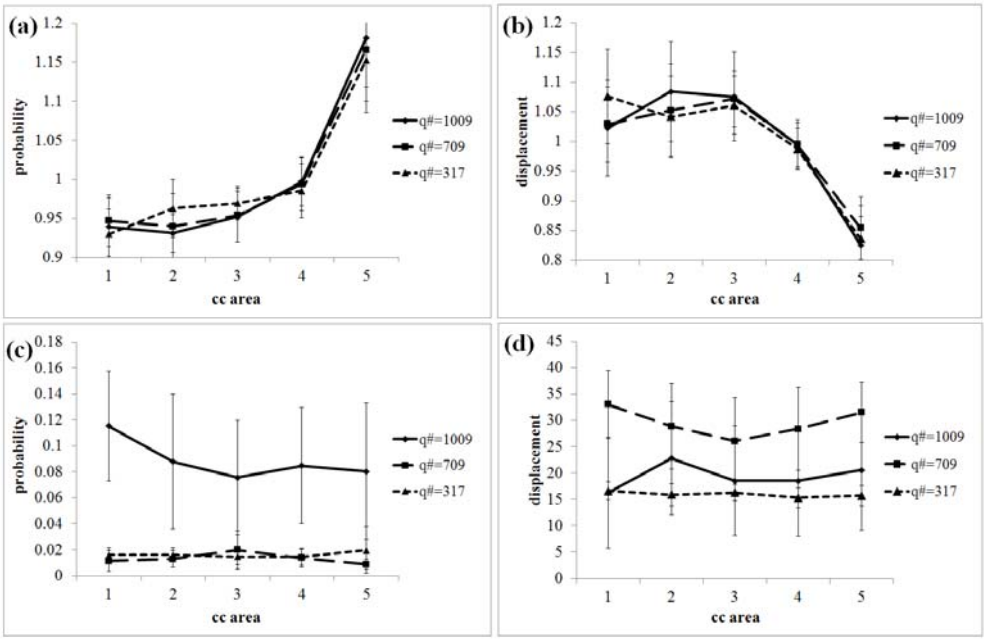

Figure 5 (a) Probability and (b) displacement distribution of CC calculated from narrow Gaussian displacement distribution with different sampling numbers in q-plane and the same cutoff b value. (c) Probability and (d) displacement distribution of CC calculated from broad Gaussian displacement distribution with different sampling numbers in q-plane and the same cutoff b value. The units in probability and displacement were arbitrary values.

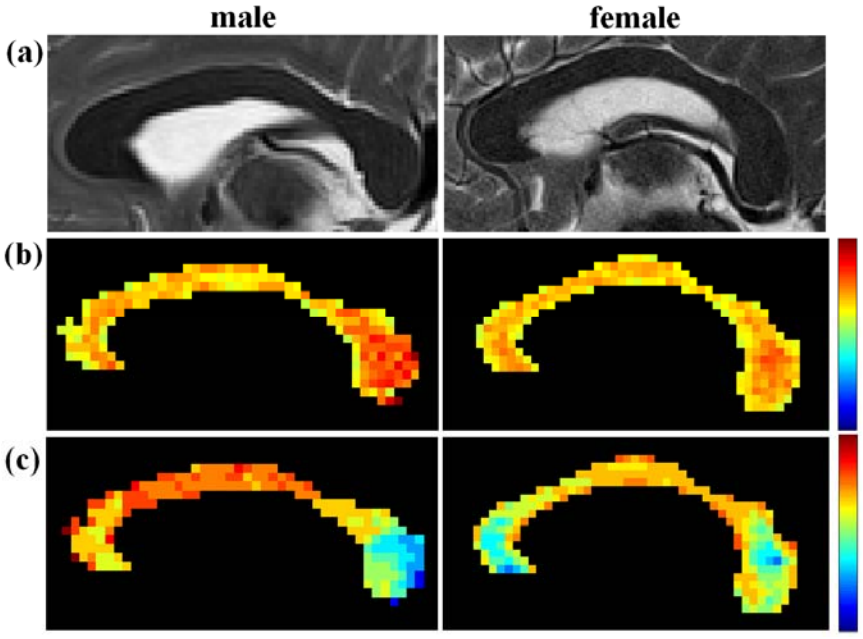

Figure 6 QPI analysis of the human CC. Sagittal indexed MRI maps of (a) T2WI, (b) probability and (c) displacement of narrow Gaussian displacement distribution in representative male (left column) and female (right column) normal subjects.

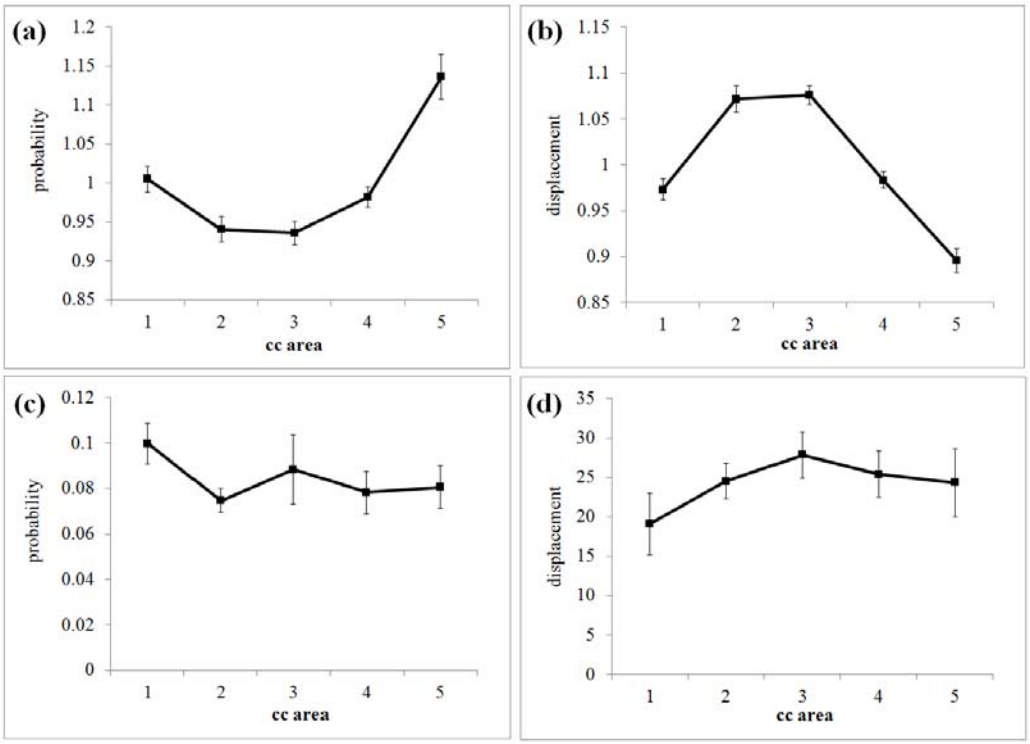

Figure 7 Axonal density and diameter distribution analysis along the human CC. Five regions of interest of mid-sagittal indexed QPI maps were selected from the five segments shown in Fig. 1. (a) Probability and (b) displacement distribution calculated from narrow Gaussian displacement distribution of CC in all normal subjects (n=14). (c) Probability and (d) displacement distribution calculated from broad Gaussian displacement distribution of CC in all normal subjects (n=14). The units in probability and displacement were arbitrary values.

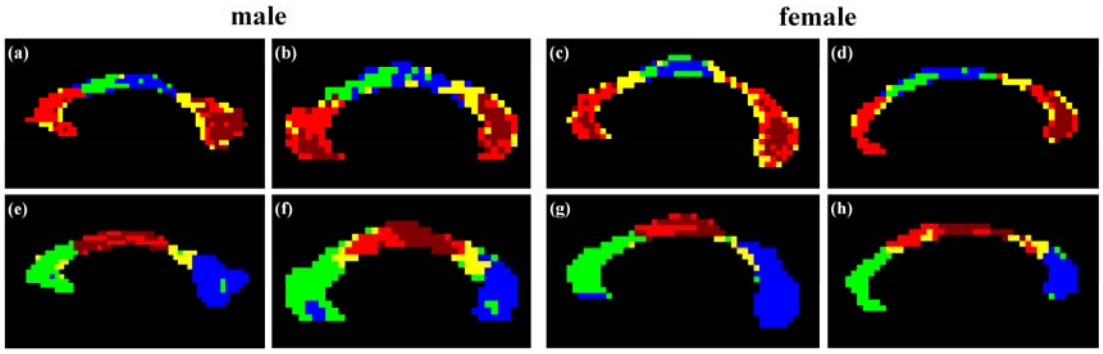

Figure 8 Cluster analysis of the axonal density and diameter distribution along the CC in four different normal subjects. Two are male (a, b, e and f) and two are female (c, d, g and h). The probability clusters are in the up row (a to d), and the displacement clusters are in the bottom row (e to h). Note that the colors of the clusters for the four subjects are matched. Also note the high similarity of the cluster pattern among the subjects.

國科會補助專題研究計畫出席國際學術會議心得報告

日期：102年 10 月 31 日

計畫編號	NSC101－2320－B－040－001		
計畫名稱	擴散波數平面磁振造影研究活體人腦胼胝體神經軸突尺寸與密度		
出國人員姓名	翁駿程	服務機構及職稱	中山醫學大學醫影系副教授
會議時間	102 年 7 月 3 日至 102 年 7 月 7 日	會議地點	日本大阪
會議名稱	(中文)第 35 屆國際生物醫學工程年會 (英文) 35th Annual International Conference of the IEEE Engineering in Medicine and Biology Society		
發表題目	(中文)雙高斯擴散波數平面磁振造影量測活體人腦胼胝體之尺寸與密度 (英文) Bi-Gaussian Q-planar MR Measurement of Axonal Diameter and Density of Human Corpus Callosum In Vivo		

一、參加會議經過

今年的國際醫工年會(35th Annual International Conference of the IEEE Engineering in Medicine and Biology Society)於7月3日到7日在日本大阪舉行，分為二個部分，包括前一日的educational courses 及後四日的scientific meeting，就醫工學會的教育及科學議程內容而言，涵蓋醫工相關基礎研究與這個學門的理論、技術及應用，以口頭或海報發表的研究在量上雖比不上北美放射年會(RSNA)或國際磁振醫學會(ISMRM)，但是涵蓋範圍廣泛，非常精彩。除了常規的口頭、壁報報告與plenary lecture之外，每天中午則有儀器或藥品等相關的廠商所舉辦的luncheon seminar，所以每天的行程可以說是相當豐富，而也因此學習到不少新知。

二、與會心得

會中接收到很多全新的觀念與技術，限於篇幅僅列舉醫療資訊方面的重點。哈佛醫學院的Dr. John Halamka提到了2009年美國歐巴馬總統開始致力於開發辦公室與醫院的電子健康記錄，並擴大醫療資訊交換，截至2013年已經投入10億美元，已經取得實質性進展與許多經驗，也分析其對其它將實施類似的計劃國家的影響。美國政府也將此醫療資訊計畫與亞洲、歐洲和加拿大相比，而醫療保健的主要趨勢將包括醫療照護應用、巨量數據分析、個人健康記錄、移動設備的電子雲、與改善其安全與

隱私。韓國三星公司高級副總裁Dr. Yoonchae Cheong則提到智慧型設備已經迅速滲透到日常生活的各種應用。隨著通訊和電腦資訊技術的進步，智慧型設備將拓展至其它領域，包括醫療保健與醫療資訊的融合。但要將真實世界到數位世界的結合更趨近完美，在許多環境設備還有很大的改進空間，包括偵測器、執行器與控制器。這些環境裝置將使用自己的網路，但又能整合於智慧型手機的基礎架構上，這將導致在許多傳統醫療保健與醫療生態系統領域的轉變。

三、發表論文全文或摘要

如附件

四、建議

感謝國科會補助教師出席國際會議發表論文，不啻觀摩並學習他人的研究成果，也藉由教育的課程提昇自己的知識面。這次在日本大阪舉辦之IEEE-EMBC會議提供我們瞭解國際在醫工領域發展的管道，並且利用出國的機會能與國際上知名的研究團隊討論及交換研究心得，是一個富有研究交流及教育訓練意義的會議。我由衷的建議國內能多鼓勵及補助教師與青年學子參與類似的會議，以達到國內科學的發展及與國際科學的接軌。

五、攜回資料名稱及內容

IEEE EMBC 2013 proceeding

六、其他

無

Bi-Gaussian Q-planar MR Measurement of Axonal Diameter and Density of Human Corpus Callosum In Vivo

Jun-Cheng Weng, Sih-Yu Lin

***Abstract*— The corpus callosum (CC) is the main fiber tract interconnecting bilateral cerebral hemispheres, and is involved in a wide variety of cognitive functions Alteration of this fiber structure has been implicated in different mental disorders. However, an in vivo technique that can map axonal diameter and axonal density of the CC is still lacking. Therefore, a new MRI method called q planar imaging (QPI) was proposed in which high density 2D diffusion encoding was performed on the mid sagittal plane of the CC.**

I. Introduction

It is known that water signal decay in a MR diffusion experiment in neuronal tissues, at sufficiently high diffusion weighting, appears to be non-mono-exponential, thus complicating even further the interpretation and assignment of the different components to actual physiological compartments [1, 2]. Therefore, we used 2D bi-Gaussian model (i.e. slow and fast components) to fit our QPI data. After 2D Fourier transformation of the slow and fast Gaussian curved surfaces of signal decay, respectively, two Gaussian curved surfaces of displacement distribution (i.e. narrow and broad components) were obtained [3]. Intracellular and extracellular information could then be extracted from the narrow and broad Gaussian displacement distributions, respectively.

II. Materials and Methods

To determine the optimal values of maximal diffusion sensitivity (b_{max}) and sampling density in the q space (Δq) for QPI on a clinical scanner, a heuristic estimation and an in vivo optimization study were performed on a healthy subject. Having known the optimal b_{max} and Δq, an in vivo validation study was performed on fourteen healthy subjects. The QPI data acquisition was performed on a 3T MR system using a diffusion-weighted spin echo EPI sequence. Multiple diffusion-weighted images were acquired corresponding to 1009 diffusion-encoding directions on a mid-sagittal plane of CC. The diffusion encoding directions corresponded to a set of 2D grid points confined in a circle with a radius of 18 increments ($\Delta q = 0.0029\ \mu m^{-1}$). The b values ranged from 0 to the optimal bmax (5000 s/mm^2). The QPI data were decomposed into fast and slow components by bi-Gaussian fitting, and 2D Fourier transform was performed on the fast and slow components of the data to obtain broad (extracellular) and narrow (intracellular) components of the 2D probability density function (PDF) of molecular displacement, respectively. Two indices of water diffusion, mean displacement and the probability density at zero displacement, were computed from the 2D PDF at each pixel to map the axonal diameter and axonal density, respectively.

III. Results

Compared with the know histology [4], bi-Gaussian QPI with optimum parameters produced reasonable distribution and segmentation of axonal diameter and density of the CC in normal human brain. The genu and splenium were significantly smaller and denser than those from other regions.

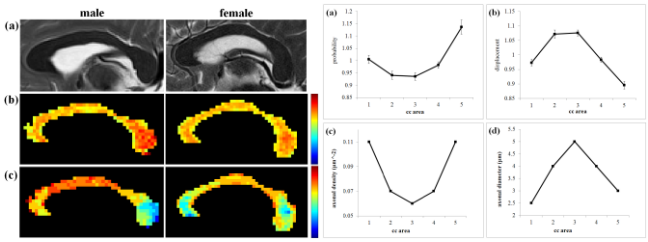

Figure 1. Left were sagittal CC mappings of (a) T2WI, (b) probability, and (c) displacement in representative male and female normal subjects. Right were (a) probability and (b) displacement distribution of CC. (c) Mean axonal density and (d) mean axonal diameter of human CC found by histology.

IV. Conclusion

Our results showed that bi-Gaussian QPI was feasible in clinical scanners, and might be potentially useful in neuroscience research and clinical application.

References

[1] T Niendorf, et al., "Biexponential diffusion attenuation in various states of brain tissue: implications for diffusion-weighted imaging," *Magn Reson Med* 1996; 36: pp. 847-57.

[2] Y Assaf, et al., "Non-mono-exponential attenuation of water and N-acetyl aspartate signals due to diffusion in brain tissue," *J Magn Reson* 1998; 131: pp.69-85.

[3] VJ Wedeen, et al., "Mapping complex tissue architecture with diffusion spectrum magnetic resonance imaging," *Magn Reson Med* 2005; 54: pp. 1377-86.

[4] F Aboitiz, et al., "Fiber composition of the human corpus callosum," *Brain Res* 1992 ; 598: pp. 143-153.

*Resrach supported in part by the research program NSC101-2320-B-040-001, National Science Council, Taipei, Taiwan.

J-C. Weng is with the School of Medical Imaging and Radiological Sciences, Chung Shan Medical University, and Department of Medical Imaging, Chung Shan Medical University Hospital, Taichung, Taiwan (corresponding author, phone: +886-4-2473-0022 ext. 12342; e-mail: jcweng@ csmu.edu.tw).

S-Y. Lin is with the School of Medical Imaging and Radiological Sciences, Chung Shan Medical University, Taichung, Taiwan (e-mail: betty810720@ yahoo.com.tw).

Preprint submitted to 35th Annual International IEEE EMBS Conference.
Received April 9, 2013.

國科會補助計畫衍生研發成果推廣資料表

日期:2013/08/07

國科會補助計畫	計畫名稱: 擴散波數平面磁振造影研究活體人腦胼胝體神經軸突尺寸與密度
	計畫主持人: 翁駿程
	計畫編號: 101-2320-B-040-001- 學門領域: 醫學工程

無研發成果推廣資料

101 年度專題研究計畫研究成果彙整表

計畫主持人：翁駿程	計畫編號：101-2320-B-040-001-
計畫名稱：擴散波數平面磁振造影研究活體人腦胼胝體神經軸突尺寸與密度	

成果項目			量化			單位	備註（質化說明：如數個計畫共同成果、成果列為該期刊之封面故事...等）
			實際已達成數（被接受或已發表）	預期總達成數(含實際已達成數)	本計畫實際貢獻百分比		
國內	論文著作	期刊論文	0	0	0%	篇	
		研究報告/技術報告	0	0	0%		
		研討會論文	10	10	80%		
		專書	0	0	0%		
	專利	申請中件數	0	0	0%	件	
		已獲得件數	0	0	0%		
	技術移轉	件數	0	0	0%	件	
		權利金	0	0	0%	千元	
	參與計畫人力（本國籍）	碩士生	2	2	90%	人次	
		博士生	0	0	0%		
		博士後研究員	0	0	0%		
		專任助理	0	0	0%		
國外	論文著作	期刊論文	2	3	80%	篇	一篇主要相關論文投稿中
		研究報告/技術報告	0	0	0%		
		研討會論文	5	5	80%		
		專書	0	0	0%	章/本	
	專利	申請中件數	0	0	0%	件	
		已獲得件數	0	0	0%		
	技術移轉	件數	0	0	0%	件	
		權利金	0	0	0%	千元	
	參與計畫人力（外國籍）	碩士生	2	2	90%	人次	
		博士生	0	0	0%		
		博士後研究員	0	0	0%		
		專任助理	0	0	0%		

其他成果 (無法以量化表達之成果如辦理學術活動、獲得獎項、重要國際合作、研究成果國際影響力及其他協助產業技術發展之具體效益事項等，請以文字敘述填列。)	指導學生洪于涵、王芸慧、吳孟穎分別獲得第八屆醫學影像暨放射科學研討會口頭報告第二名、壁報論文第三名、壁報論文佳作 指導學生林思妤、王惠瑜、吳孟穎獲得 102 學年度國科會補助大專學生參與專題研究計畫

	成果項目	量化	名稱或內容性質簡述
科教處計畫加填項目	測驗工具(含質性與量性)	0	
	課程/模組	0	
	電腦及網路系統或工具	0	
	教材	0	
	舉辦之活動/競賽	0	
	研討會/工作坊	0	
	電子報、網站	0	
	計畫成果推廣之參與（閱聽）人數	0	

國科會補助專題研究計畫成果報告自評表

請就研究內容與原計畫相符程度、達成預期目標情況、研究成果之學術或應用價值（簡要敘述成果所代表之意義、價值、影響或進一步發展之可能性）、是否適合在學術期刊發表或申請專利、主要發現或其他有關價值等，作一綜合評估。

1. 請就研究內容與原計畫相符程度、達成預期目標情況作一綜合評估

■達成目標

□未達成目標（請說明，以 100 字為限）

□實驗失敗

□因故實驗中斷

□其他原因

說明：

2. 研究成果在學術期刊發表或申請專利等情形：

論文：□已發表 ■未發表之文稿 □撰寫中 □無

專利：□已獲得 □申請中 ■無

技轉：□已技轉 □洽談中 ■無

其他：(以 100 字為限)

3. 請依學術成就、技術創新、社會影響等方面，評估研究成果之學術或應用價值（簡要敘述成果所代表之意義、價值、影響或進一步發展之可能性）(以 500 字為限)

我們成功的建立擴散波數平面造影(q-planar imaging, QPI)來偵測活體人腦胼胝體的神經軸突尺寸與密度。而此平台的建立是相當具有前瞻性的醫學研究，以及臨床應用與醫療市場產業價值。我們的研究結果已經發表數篇國內外研討會論文，也將發表為國際期刊論文。這些成果對於腦神經科學研究、精神醫學研究、結構性磁振造影等科學具有所參考價值，並可提高本校與本院醫學研究水準。參與研究之人員可學習擴散磁振造影系統基礎理論、技術、影像分析之能力，以及研發新的造影技術，瞭解建立平台時所面臨之問題，培養解決問題的能力，這些訓練對於從事醫學影像研究者而言非常重要。並藉由本實驗學習結構性磁振造影的操作與分析，並可將這些相關技術應用在其它疾病的磁振造影的研究，同時了解一個研究計畫的執行過程以及如何將實驗成果做到最有價值的運用。未來可將此分析平台應用於評估胼胝體受到疾病進程發展、大腦認知功能、左右半腦交通損傷等因素影響，其結構改變，幫助相關疾病進展與治療前後的評估，並且可進一步探索或研發神經科學研究與臨床疾病診斷相關技術與醫儀器材，進而提升國內醫療品質、民眾福祉與醫療相關研究之發展。